Planta (2008) 229:15–24
DOI 10.1007/s00425-008-0799-9

ORIGINAL ARTICLE

Compositional characterization and imaging of "wall-bound" acylesters of *Populus trichocarpa* reveal differential accumulation of acyl molecules in normal and reactive woods

Jin-Ying Gou · Simone Park · Xiao-Hong Yu · Lisa M. Miller · Chang-Jun Liu

Received: 14 July 2008 / Accepted: 22 July 2008 / Published online: 27 September 2008

Abstract Acylesterification is one of the common modifications of cell wall non-cellulosic polysaccharides and/or lignin primarily in monocot plants. We analyzed the cell-wall acylesters of black cottonwood (*Populus trichocarpa* Torr. & Gray) with liquid chromatography–mass spectrometry (LC–MS), Fourier transform-infrared (FT-IR) microspectroscopy, and synchrotron infrared (IR) imaging facility. The results revealed that the cell wall of dicotyledonous poplar, as the walls of many monocot grasses, contains a considerable amount of acylesters, primarily acetyl and *p*-hydroxycinnamoyl molecules. The "wall-bound" acetate and phenolics display a distinct tissue specific-, bending stress responsible- and developmental-accumulation pattern. The "wall-bound" *p*-coumarate predominantly accumulated in young leaves and decreased in mature leaves, whereas acetate and ferulate mostly amassed in the cell wall of stems. Along the development of stem, the level of the "wall-bound" ferulate gradually increased, while the basal level of *p*-coumarate further decreased. Induction of tension wood decreased the accumulation of the "wall-bound" phenolics while the level of acetate remained constant. Synchrotron IR-mediated chemical compositional imaging revealed a close spatial distribution of acylesters with cell wall polysaccharides in poplar stem. These results indicate that different "wall-bound" acylesters play distinct roles in poplar cell wall structural construction and/or metabolism of cell wall matrix components.

J.-Y. Gou · X.-H. Yu · C.-J. Liu (✉)
Department of Biology, Brookhaven National Laboratory, Upton, NY 11973, USA
e-mail: cliu@bnl.gov

S. Park · L. M. Miller
National Synchrotron Light Source, Brookhaven National Laboratory, Upton, NY 11973, USA

Keywords Acylesterification · Chemical imaging · *Populus trichocarpa* · "Wall-bound" phenolics · Tension wood

Abbreviations

FT-IR	Fourier-transform infrared
IR	Infrared
LC–MS	Liquid chromatography–mass spectrometry
GalA	Galacturonic acid

Introduction

Plant cell wall provides mechanical strength to vascular plants and represents the most abundant renewable biomass potentially for biofuel production. During cell-wall biogenesis and modification, several types of acylesterifications, including acetylation and *p*-hydroxycinnamoylation, occur on the wall matrix components, non-cellulosic polysaccharides, lignin, and perhaps, the wall-associated structural proteins (Fry and Miller 1989; Iiyama et al. 1994; Hatfield et al. 1999). Certain cell wall polysaccharides, notably, arabinoxylan in graminaceous plants (tropical perennial grasses) and pectin of spinach and sugar beets are substituted with phenolic esters involving *trans*-feruloyl and *trans-p*-cinnamoyl groups (Fry 1986; Ishii 1997a). Feruloyl groups in the gramineas are mainly substituted at position *O*-5 of the α-L-arabinofuranoyl residues, which then are attached to the *O*-3 position of β-1,4-linked D-xylose in the backbone of hemicellulose (Wende and Fry 1997a; Ishii 1997a). Through a peroxidase-catalyzed dimerization or an ether-to-ester linkage, these so-called "wall-bound" phenolics can form complex cross-links between polysaccharides, polysaccharide and lignin, and, probably, polysaccharide and structural protein (Bunzel et al. 2004; Ralph et al. 2004;

Piber and Koehler 2005). The cross-linkages of wall polymers mediated by phenolic esters may significantly stabilize the three-dimensional structure of the cell wall matrix and facilitate the formation of wall-matrix network for imbedding cellulose microfibrils. Such cross-linkages also limit the accessibility of polysaccharide hydrolases to their substrates, and hence, hinder microbial degradation of cellulosic fibers (Kato and Nevins 1984; Grabber et al. 2004). In addition to feruloylation of cell-wall polysaccharide hemicellulose or pectin, lignin in many monocot crops and woody plants are frequently esterified with *p*-hydroxybenzoyl, or *p*-coumaroyl moieties (Sederoff et al. 1999; Lu and Ralph 1999; Lam et al. 2001; Lu and Ralph 2002). These different acylesterifications are believed to occur in monolignols by γ-linkage, and incorporated into lignin during polymerization. The acyl moieties of lignin may also function as inter- or intra-molecular cross-linkers to connect lignocellulosic polymers, or as the special electron-transfer carrier during oxidative coupling for lignin polymerization (Ralph et al. 2004). Besides aromatic acylation, cell wall polysaccharides, hemicellulose and pectin, and lignin also undergo significant *O*-acetylation (Wende and Fry 1997b). A high degree of acetylation on pectin, a primary cell wall component, was noted in several important crops, such as potato and sugar beet (Liners et al. 1994; Schols and Voragen 1994; Ishii 1997b; Renard and Jarvis 1999). The extent of *O*-acetylation of GalA residues in pectin varies from 0 to 90% depending on the particular tissue, and species (Schols and Voragen 1994; Voragen et al. 1998). Although the role of such *O*-acetylation of polysaccharide backbones *in planta* is unclear, the *O*-acetyl substituents on pectin may affect the solubility and gelatability of pectin (Pippen et al. 1950; Rombouts and Thibault 1986). Moreover, acetylesters of cell wall polysaccharides may act as physical barrier hindering the enzymatic breakdown of polysaccharide polymers (Biely et al. 1986; Tenkanen 1998; Renard and Jarvis 1999).

Cell wall acylesterification, therefore, likely contributes the wall recalcitrance to hydrolysis thus reducing the degradability of lignocellulosic biomass. Understanding the biogenesis and regulation of cell wall acylesterifcation in "biogenergy" crops will facilitate manipulating cell wall's biochemical and biophysical properties, thus improving the conversion of lignocelluloses to biofuel.

Poplars are a fast growing dicotyledonous woody species. The wood of *Populus* spp. consists of about 50% cellulose, 30% hemicellulose, and 20% lignin, representing one of the most promising bio-resources providing carbohydrate biomass for biofuel production (Aspeborg et al. 2005). The whole genome sequencing of black cottonwood (*Populus trichocarpa* Torr. & Gray), the one of poplar species, was recently completed (Tuskan et al. 2006), which provides profound molecular resource to study cell wall biogenesis and modification. Being interested in characterizing the molecular factors controlling lignocellulosic structural properties of wood species, and eventually manipulating wood feedstock's digestibility to facilitate biofuel production, we took black cottonwood as our model experimental system. As acylesterification was mostly reported from the cell wall of monocot grass species, so the first step, we examined whether cell wall of black cottonwood undergoes similar acylesterific modifications. To do that we adopted FT-IR, synchrotron IR spectroscopic chemical imaging and LC–MS techniques. Our results revealed that three major types of acylesters, i.e., acetyl, *p*-coumaroyl, and feruloyl moieties were abundant in black cottonwood cell wall alkali extractable fractions; the spatial distribution of acylesters in poplar wood tissues correlates well with cell wall polysaccharides; the accumulation of those "wall-bound" acylesters exhibit clear tissue-specific pattern and the levels of the accumulated acylesters differentially changed along plant development and in response to bending stress. These data implicate the distinct functions of acylesters in poplar cell wall architecture and metabolism of cell wall components.

Materials and methods

Chemicals

The authentic polysaccharides, cotton cellulose and beech wood xylan, in FT-IR study and the authentic phenolic compounds, ferulic acid, *p*-coumaric acid, caffeic acid, etc., used in LC–MS analysis were purchased from Sigma-Aldrich (St Louis, MO).

Plant material and sampling

Plantlets of *Populus trichocarpa* L. (black cottonwood), about 1-year-old, were purchased from Oak Point Nursery (Indepence, OR) and grown in greenhouse at 22°C on March of 2006. The leaves and stem internodes were collected on October, 2006. The internodes were counted from the shoot tip. The leaves on the shoots were pooled into three groups. The unexpanded leaves from shoot tip represent the young leaves. The fully expanded leaves from developing shoot (between nodes 5 to ~26) represent the mature leaves, and the leaves on the node 26 below displayed senescent symptom thus were grouped as old leaves. All materials were collected and immediately frozen using liquid N_2 and stored at −80°C.

Arabidopsis thaliana wild type (Col-0) was grown in a growth chamber at 22°C with 14 h light/10 h dark regime for about 2 months, and the leaves and stems were collected to serve as controls to validate the FT-IR and LC–MS methods in examining the cell wall compositions.

Induction of poplar tension wood

To induce poplar tension wood (TW), about 2-year-old polar plantlets were transferred to growth chamber (at 22°C with 14 h light/10 h dark regime). At the onset of cambium growth at early spring (March 2008), the shoot around internodes 9–15 were artificially bended into an arch for 3 weeks, and the developing secondary xylem from the upper portion (TW) of the bent segments were collected. The segments of the internodes 9–15 of the adjacent shoots within the same plantlet were collected as control. Three independent treatments were conducted with different plantlets.

Alkaline hydrolysis of cell wall and analysis of released wall-bound acylesters

The leaves and stems of black cottonwood and *Arabidopsis* were ground into powder under liquid N_2. The ground powder of different tissues were extracted sequentially with 70% ethanol at 75°C for 1 h three times, and then with methanol:acetone (1:1) three times at room temperature. Since caffeic acid normally does not present as a "wall-bound" phenolic, it was mixed into the powdered tissues serving as internal standard to monitor the efficiency of removing soluble compounds and to determine cell-wall composition free from soluble chemicals. The extract residues were thoroughly washed by acetone and then with water, and vacuum-dried at 40°C. When the cell wall samples were prepared for FT-IR analysis, an amount of the dried residues was first extracted with 20 mM ammonium oxalate at 70°C three times, then washed with water, and the residuals were subsequently hydrolyzed with 2 N NaOH at room temperature overnight. The insoluble fractions at each step were subjected to FT-IR analysis. When cell wall extracts were used for LC–MS characterization, the dried ethanol-free cell wall fraction was directly taken to alkali hydrolysis without ammonium oxalate treatment, and 4-methoxycinnamic acid was added as internal standard. The hydrolysates were acidified with 6 N HCl to pH 3.0, and acetate contents of a portion of acidified hydrolysates were determined using the Acetic Acid Detecting Kit (Megazyme, Co. Wicklow, Ireland) by following manufacturer's procedures. Quantification was based on the standard curve generated using the same batch of assay kit with acetic acid standard. The remaining hydrolysates were extracted with water-saturated ethyl acetate three times. After pooling and drying ethyl acetate extracts, the residuals were redissolved in methanol and detected by LC–MS for "wall-bound" phenolics.

The prepared sample was injected into a C18 reverse-phase column (Gemini, 5 μm, 4.6 × 250 mm, Phenomenex) and resolved in 0.2% acetic acid (A) with an increasing concentration gradient of acetonitrile containing 0.2% acetic acid (B) for 0–5 min, 5%; 5–9 min, 17%; 9–10 min, 17%; 10–22 min, 21%; 22–40 min, 23%; and, 40–60 min, 50% at a constant rate of 1.0 ml/min. UV absorption was monitored at 260-, 280-, 310-, and 510-nm with a multiple wavelength photodiode array detector. The half amount of HPLC fluent was directly injected into a tandem linked LC/MSD Trap XCT system equipped with an Electron Spay Ionization source (Agilent technologies, Santa Clara, CA) for MS analysis. The full range of total ion chromatogram (50–1,000 m/z) was acquired under negative mode with parameter setting of nebulizer 50 psi, dry gas 10 l/min, dry temperature at 300°C and compound stability at 10%.

The MS spectra of each particular peak were extracted for characterizing the resolved metabolites. Quantification of the identified "wall-bound" phenolics was based on the detected area of UV absorbance. The areas of UV absorptive peaks at 310 nm for the resolved *p*-coumarate and ferulate were first normalized with that of the internal standard, then calibrated with the standard curves generated from authentic *p*-coumarate and ferulate that resolved with the same HPLC method under the same wavelengths. The quantification of the putative dehydroferulic/coumaric dimers was based on the ferulate standard curve.

Synthesis of acetylated xylan

To synthesize the acetylated xylan standard for FT-IR study, 1 g beech wood xylan (Sigma) as suspended in formamide at ~20 mg/ml at 50°C for 1 h, then 20 ml pyridine was added and carefully mixed. After cooling the mixture down to the room temperature, 15 ml acetic anhydride was added drop-wise into the mixture with gently shaking for 2 h allowing occurrence of the acetylation reaction. Subsequently, the reaction mixture was thoroughly dialyzed against water at 4°C for 2 days to remove the unbounded acetic residues. The final concentration of the acetyl attached on xylan polymer was determined using the Acetic Acid Detecting Kit (Megazyme, Co.) The degree of acetylation of the xylose residues in the polymer is about 22% (mol/mol).

FT-IR microspectroscopy

FT-IR microspectra were collected from the fresh leaf and/or stem, and the insoluble fractions of black cottonwood and *Arabidopsis* cell walls at each extraction step, as described above. The ethanol extract-free residues and the dried residues after alkaline treatment were rehydrated with water. Approximately 1–2 μl of the resultant slurry was pipetted onto a BaF_2 microscope slide, allowed to dry, and scanned with a Perkin Elmer Spectrum Spotlight IR microscope (Waltham, MA) in "point" mode. The IR beam size was set to 50 μm, and five spectra were collected from

different regions of each dried droplet. Spectra were collected from 4,000 to 720 cm^{-1} in transmission mode at 8 cm^{-1} resolution and averaged to obtain the final results.

Synchrotron infrared imaging

For synchrotron infrared imaging of the poplar stem section, a piece, 1-cm long, was cut from the stem within the first five internodes and flash-frozen in liquid nitrogen. The specimen was mounted in Tissue-Tek freezing medium, and sectioned with a cryomicrotome (Leica Microsystems, Wetzlar, Germany) at −20°C. Sections (7 μm thick) were placed on a BaF_2 microscope slide and dried at room temperature. IR images were collected using a Perkin Elmer Spectrum Spotlight FTIR Imaging System (Waltham, MA) operated in the "image" mode of the instruments using a 6.25 μm pixel resolution. The instruments was equipped with a liquid nitrogen-cooled mercury cadmium telluride (MCT-A) array detector, and an automated mapping stage. For each tissue section, a light micrograph was obtained, and the regions to be imaged with the IR microscope were defined. Infrared images were collected in transmission mode by raster-scanning the sample through the IR beam and collecting infrared absorbance spectra at each pixel. For each pixel, an entire infrared spectrum is obtained from 4,000 to 720 cm^{-1}. Background spectra were gathered from a clean region of the BaF_2 slide. The spectral resolution was 8 cm^{-1} and 16 scans were averaged for each spectrum. From each FT-IR dataset, various spectra regions were integrated to generate images of the distributions of different chemical components: aromatics (3,250 cm^{-1}), oils and waxes (2,915 cm^{-1}), (acyl)ester groups (1,740 cm^{-1}), protein (1,650 cm^{-1}), lignin (1,510 cm^{-1}), and polysaccharides (1,070 cm^{-1}).

Results

FT-IR analysis of wall-bound esters of poplar lignocelluloses

Poplar stems and leaves were sequentially extracted with hot ethanol and acetone, and the extract-free residues then hydrolyzed with alkali solution. These treatments generated the collections of the total cell-wall fraction (ethanol extract-free residues), non-cellulosic polysaccharides, primarily hemicellulose fraction (alkali hydrolysate), and the remaining cellulose–lignin complex fraction. Since phenolic esters have been detected on the cell wall of *Arabidopsis* previously (Franke et al. 2002), *Arabidopsis* rosette leaves and stems were also treated in the same way as positive control to validate the detection method. We subjected the ethanol extract-free residues of poplar and *Arabidopsis* leaves and stems to FT-IR spectroscopy before and after alkaline treatment. All spectra from poplar and *Arabidopsis* leaf and stem cell wall fractions showed numerous overlapping absorption bands for polysaccharides between 800 and 1,200 cm^{-1} (Marchessault and Liang 1962; Robert et al. 2005) (Fig. 1a, b), which are largely identical to those spectra recorded from purified cellulose and hemicellulose standards (Fig. 1c). A major absorption band around 1,040–1,070 cm^{-1} with a shoulder at 985 cm^{-1} might be assigned to C–OH bending. The absorption band around 1,150 cm^{-1} was assigned to glycosidic linkages, while the small band around 890 cm^{-1} was characteristic of β-(1–4) linkages (Fig. 1) (Robert et al. 2005; Philippe et al. 2006). An absorption peak around 1,510 cm^{-1}, representing aromatic ring in lignin polymer, was present primarily in cell walls of poplar stem. The absorption bands around 1,640 cm^{-1} were overlapped with the amide I vibration, which may derived from some proteins that remained in the ethanol-treated residues, and the vibrations of uronic acid carboxylate and residual water, as well as the aromatic vibration in the case of low lignin content samples (Kacuráková et al. 1999, 2000). Besides these characteristic bands, a strong IR absorption band was observed at 1,740 cm^{-1} in all of the stem and leaf ethanol extract-free cell-wall samples before alkaline hydrolysis (Fig. 1a1, a3, b5, b6), but was mostly absent from the saponified samples (Fig. 1a2, a4, b7), in which non-cellulosic polysaccharides and their substituents had been removed (Fry 1986). The peak at 1,740 cm^{-1} is assigned to the characteristic feature of carboxylic-ester bonding (C=O) (McCann et al. 2001; Robert et al. 2005). To confirm that this vibration reflects acylester bonding, we chemically acetylated the β-(1-4)-D-xylan polymer from beech wood; this acetylated xylan showed a strong identical IR absorption at 1,740 cm^{-1} (Fig. 1c), which was absent in the pure β-(1-4)-D-xylan authentic standard (Fig. 1c). These results suggest that considerable esterification occurs on the cell wall alkali-extractable polysaccharides of both poplar and *Arabidopsis*, and alkaline treatment hydrolyzes those esters from the cell wall.

In situ distribution of acylester compositions

The high spatial resolution of a synchrotron IR source permits in situ mapping of chemical compositions in plant tissues and cells (Miller and Dumas 2006). Cross-sections (Fig. 2a, ~7 μm thick) of the young stems of poplar (around 5th–9th nodes) were cut on a cryo-microtome and infrared images were collected with an IR microscope in the transmission mode by raster-scanning the sample through the IR beam. By integrating specific spectral features (Fig. 2b), we obtained the distributions of different chemical compositions. In poplar developing stem, most polysaccharides, represented by C–OH bending at 1,740 cm^{-1}, were

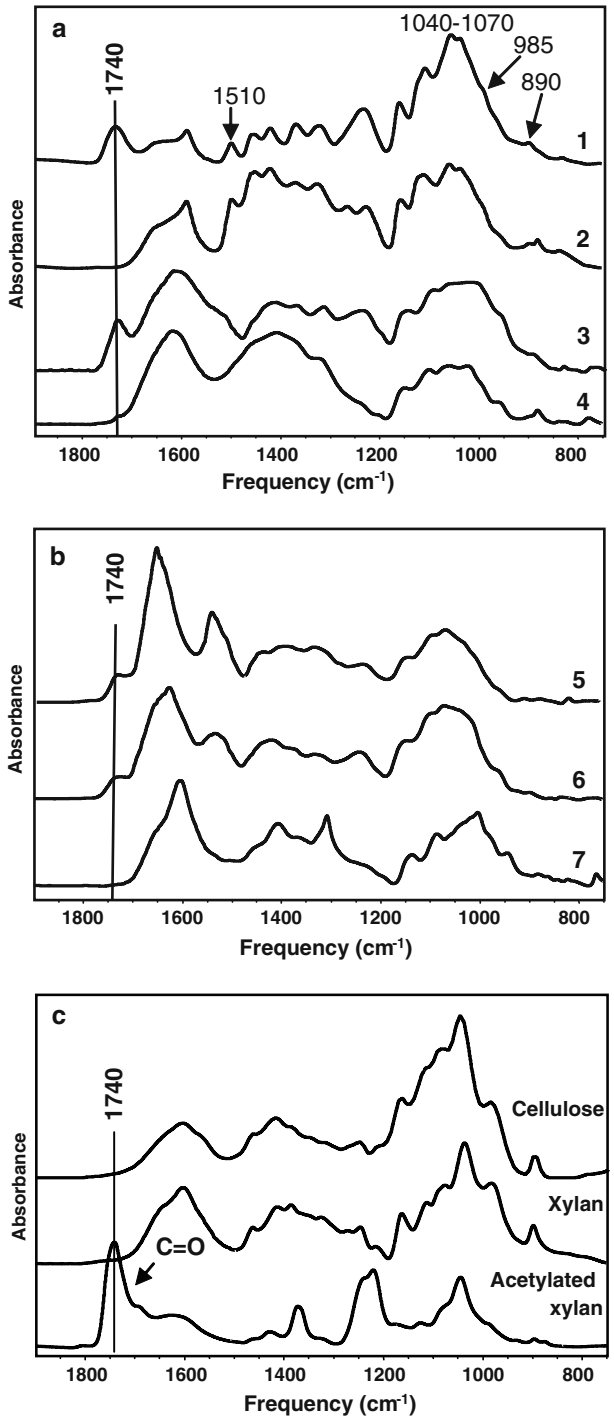

Fig. 1 FT-IR microspectra of the cell wall components. **a** The averaged FT-IR spectra of the cell walls of *P. trichocarpa* stems before (*1*) and after (*2*) alkaline treatment, and of the leaves before (*3*) and after (*4*) alkaline treatment. **b** The averaged FT-IR spectra of *Arabidopsis* fresh leaves (*5*), the cell wall fractions of the leaves before (*6*) and after (*7*) alkaline treatment. **c** The averaged FT-IR spectra of authentic cotton cellulose, beech wood xylan and chemically acetylated xylan standards

observed in the vascular xylem (woody tissue) (Fig. 2c), consistent with their role in cell-wall building. In accordance with polysaccharide allocation, a moderate level of esters with characteristic IR absorption at 1,740 cm^{-1} were observed in the same tissues and exhibit a similar distribution pattern with that of polysaccharide, thereby highlighting the co-localization of the cell-wall polysaccharide components and the IR-detected esters in xylary tissues (Fig. 2c). The newly developing stem exhibited a low level of lignification; a moderate level of lignin polymers accumulated and was deposited among vascular tissues. In addition, large amounts of aromatics, oils, and waxes built up in the epidermis and the cortex parenchyma cells, implying the potential roles of these compounds in defense responses and protecting plants from environment stresses. Aromatic compounds and oils were also observed around cell wall of vessel element, vascular fiber and ray parenchyma cells that radiated in the xylem (Fig. 2c). During the formation of wood in many trees species, different metabolites, including phenolics, are synthesized in sap wood cell and are deposited in lignified vascular tissues for disease resistance and imparting characteristic wood texture, color, etc., (Croteau et al. 2000).

Tissue-specific and developmental accumulation of wall-bound" acylesters

To further characterize and quantify the acyl moieties bound on the cell walls of poplar, the extractive-free cell wall fractions of black cottonwood leaves and stems under different growth stages were treated with alkaline. After acidifying alkali hydrolysates, aliquots of the extract were taken to determine acetyl content; the remaining extract was partitioned with organic solvent and analyzed by LC–MS.

The high amount of "wall-bound" acetate that released by saponification was detected in the hydrolysates of both poplar leaf and stem cell-wall fractions (Fig. 3). The levels of those "wall-bound" acetyl molecules in different development stages of leaves and stems exhibit large variation. The overall content of the "wall-bound" acetate was higher in the stem than that in the leaf (Fig. 3). The developing stem, representative of the nineth internodes, accumulated about 270 μmol/g cell wall dry weight of acetate, which is much higher than did the older parts of the stem (37th and 41st internodes) (Fig. 3).

Similar to that observed in monocot species, the "wall-bound" phenolics resolved from alkali extracts of poplar leaf and stem cell wall by LC–MS were predominantly *trans-p*-coumarate and *trans*-ferulate (Fig. 4a–d). Two major peaks in the UV profiles of leaf or stem extract yielded the mass spectra with a predominant ion of 163.3 and 193.7 m/z, corresponding to the *trans-p*-coumarate and *trans*-ferulate, respectively. In addition, their retention time and UV-spectra are identical to the authentic standards (data not shown). A chromatographic peak corresponding

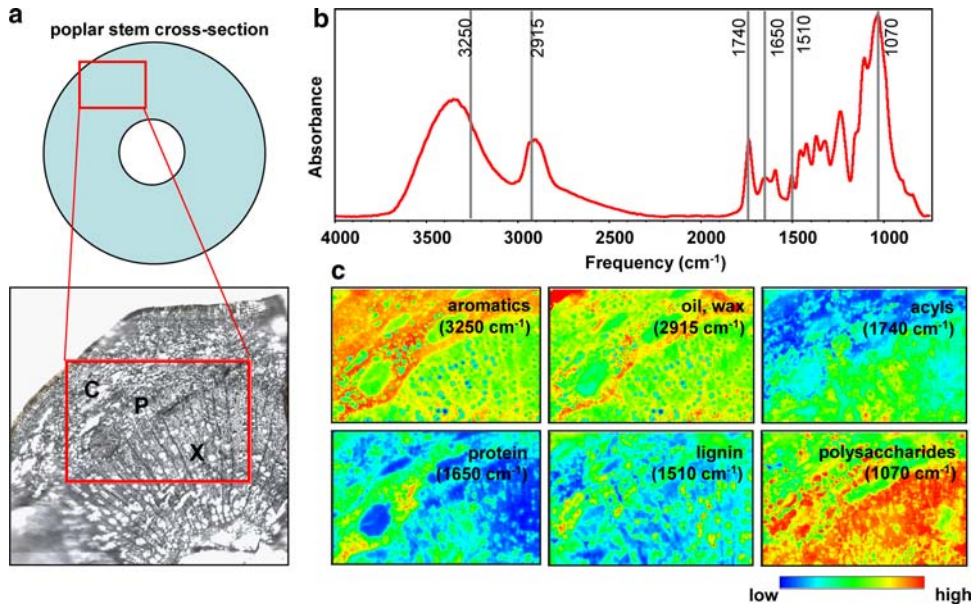

Fig. 2 Infrared imaging of a cross-section of poplar stem. **a** Schematic and light micrograph of transverse section of poplar young stem. The frame illustrates the region imaged with the IR microscope. **b** Typical IR spectrum of a poplar stem with absorptions of the interests labeled: *aromatics* (3,250 cm^{-1}), *oils* and *waxes* (2,915 cm^{-1}), *acyl* groups (1,740 cm^{-1}), *protein* (1,650 cm^{-1}), *lignin* (1,510 cm^{-1}), and *polysaccharides* (1,070 cm^{-1}). **c** Infrared images of the chemical compositions in poplar stem cross-section. The distribution of each composition was generated by integrating the peaks centered at characteristic IR absorption. The content was shown as heat-map. *C* cortex, *P* phloem, and *X* xylem

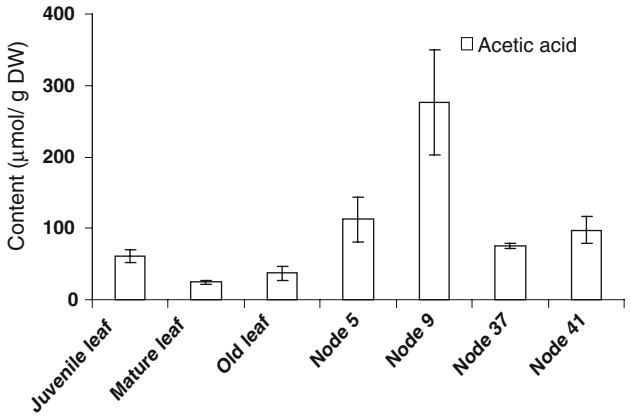

Fig. 3 Acetylester content of alkaline hydrolysates of poplar leaves and stems in different growth stages. Juvenile leaves are those unexpanded leaves attached on the node immediately under shoot apex; mature leaves are from developing stems (from 1 to ~26 internodes); old leaves are the leaves showing senescent symptom on the developed stems. *DW* dry weight of cell wall

to *cis*-*p*-coumarate was also resolved in the profiles of cell wall alkali hydrolysates of both poplar leaves and stems. This product is probably due to the non-specific conversion from *trans*-configuration of the coumarate during saponification treatment (Franke et al. 2002). In addition, trace amount of *p*-hydroxybenzate (data not shown), vanillin, and putative ferulic or *p*-coumaric dehydrodimers also were detected (Fig. 4d).

Similar to acetate, the "wall-bound" ferulate ester was mainly detected in the stem, whereas *p*-coumarate was predominant in the hydrolysate of the leaf cell wall (Figs. 4, 5). In the cell wall of unexpanded juvenile leaves, the average amount of *p*-coumarate reached up to 2.9 µmol/g cell wall dry weight, and this amount was decreased in the mature and senescent leaves (Figs. 4a, b, 5), whereas, the level of ferulate remained constant in the cell walls of young and old leaves and the average level of ferulate was about 8–10 times lower than that of *p*-coumarate (Figs. 4a, b, 5). However, in the stem the accumulation of ferulate clearly increased with wood development, and the level of ferulate accumulated in the wood changed from 0.4 µmol/g dry weight in the internode 5 to 1.3 µmol/g dry weight in the internodes 37 and 41; meanwhile, the putative dehydroferulic/coumaric dimers also slightly increased from about 0.14 µmol/g dry weight of cell wall in the early developing stem to about 0.3 µmol/g in the old stem; whereas, *p*-coumarate largely declined from 0.8 to 0.15 µmol/g cell wall dry weight (Figs. 4c, d, 5).

Accumulation of "wall-bound" acylesters in tension wood

The "wall-bound" acylesters of tension wood alkali hydrolysates were also analyzed by LC–MS and colorimetric assay. The compositions of the "wall-bound" phenolics in the tension wood were much similar to those of the control xylem tissues (data not shown), but the accumulated levels

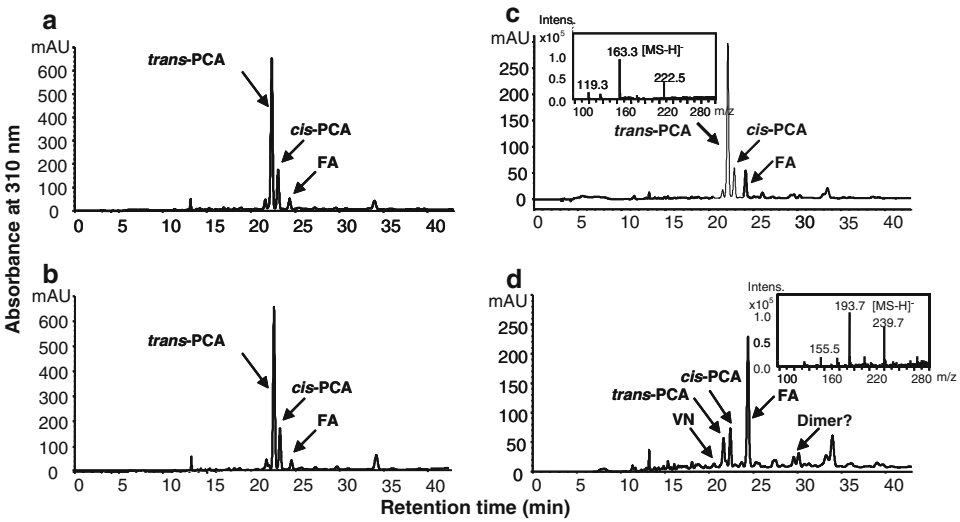

Fig. 4 UV–HPLC–ESI-MS profiles of the "wall-bound" phenolics from the cell wall fractions of the poplar unexpanded (**a**) and mature (**b**) leaves and the stems of node 5 (**c**) and node 37 (**d**). *Insets* show mass spectra of two major compounds, *trans-p*-coumarate (*trans-PCA*) and ferulate (*FA*). The other compounds are *cis-p*-coumarate (*cis-PCA*), vanillin (*VN*) and putative dehydroferulate/coumarate dimers

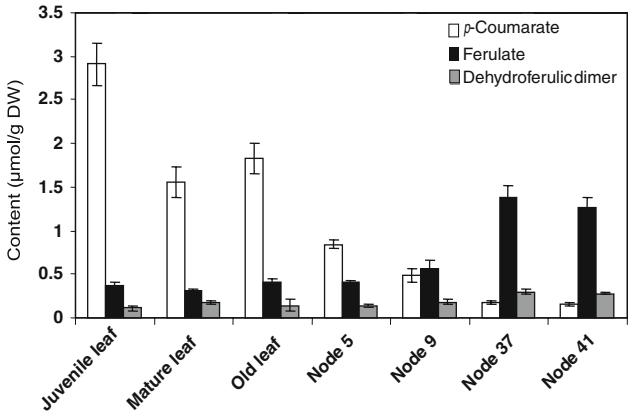

Fig. 5 The "wall-bound" *p*-coumarate, ferulate and the putative ferulate/coumarate dehydrodimer content of alkali hydrolysates of poplar leaves and stems in different growth stages. *DW* dry weight of cell wall

Table 1 Content of the "wall-bound" acylesters from alkali hydrolysate of poplar tension wood

	p-Coumarate* (nmol/g DW)	Ferulate* (nmol/g DW)	Acetate (μmol/g DW)
Control	413.2 ± 48.7	457.2 ± 58.7	203.5 ± 13.4
Tension wood	293.2 ± 39.1	289.6 ± 98.9	197.0 ± 11.3

The values represent the mean and standard deviation of three replicates for phenolics and two replicates for acetate, and each replicate with triplicate determinations

DW dry weight of cell wall

* The *t* test *P* value < 0.01

of those "wall-bound" acylesters were differentially changed (Table 1). In the control tissues, the levels of the "wall-bound" *p*-coumarate were about 413 nmol/g dry weight of cell wall, and of ferulate were about 457 nmol/g (Table 1), whereas, in the tension wood, both *p*-coumarate and ferulate were obviously declined, and more than 30% decrease was observed in the cell walls of the bending-treated samples, compared to the controls. The total content of the "wall-bound" acetate, however, remained unchanged in the tension woods and the normal developing woods (Table 1).

Discussion

Non-cellulosic polysaccharides and lignin polymers of plant cell wall exhibit different types of acylesterifications. The predominant acylesters detected from alkali extract of cell wall of black cottonwood (*P. trichocarpa*) are both acetyl- and *p*-hydroxycinnamoyl-moieties (primarily *p*-coumaroyl and feruloyl) (Figs. 3, 4, 5). Detection of acetyl group in poplar cell wall non-cellulosic fraction is consistent with the previous structural characterization of the hemicelluloses present in wood species. Acetylated hemicelluloses were found both in softwood species, such as spruce, and in hardwood species, such as aspen (Timell 1964, 1969; Teleman et al. 2000; Jacobs et al. 2002). The major constituent of the hemicellulose of softwood is an *O*-acetyl-(galacto)-glucomannan, with a minor proportion of arabino-4-*O*-methylglucuronoxylan. In the case of hardwood, the predominant component of the hemicellulose is an *O*-acetyl-(4-*O*-methylglucurono)-xylan, also called acetylated 4-*O*-methylglucuronoxylan, together with small amounts of glucomannan (Timell 1969; Teleman et al. 2000, 2003; Jacobs et al. 2002). Many xylose- or mannose-residues in such hetero hemicellulosic backbones are modified with the *O*-acetyl group at C-2 and/or C-3 positions. Acetylation also was reported to occur on the primary cell wall component pectin, e.g., homogalacturonan and rhamnogalacturonan I in several crop species (Ishii 1997b). The roles of the *O*-acetyl substituents in vivo is not fully

understood, but in vitro digestion experiments on the *O*-acetylated xylan (Biely et al. 1986), xyloglucan oligosaccharides (Pauly et al. 1999), homogalacturonan (Renard and Jarvis 1999), and rhamnogalacturonan I (Kauppinen et al. 1995) suggest that one of their functions might be the involvement in the hindrance of enzymatic polysaccharide breakdown. *O*-acetyl substituents also affect the solubility and gelation property of pectin (Pippen et al. 1950; Rombouts and Thibault 1986); partial hydrolysis of acetyl esters in beet pectin leads to an improvement of the gelation properties (Williamson et al.1990), and deacetylation makes pectin more soluble in water by decreasing the pectin backbone hydrophobicity. In addition, the degree of *O*-acetylation might be a structural factor for the development of cell wall physical properties. The degree of *O*-acetylation can change during growth and differentiation of plant tissue, which was observed in sugar-beet calli (Liners et al. 1994). Similarly, the content of acetylester of poplar's non-cellulosic polysaccharides exhibits fluctuations during the development of leaf and stem (Fig. 3). The acetylesters detected from the cell wall of black cottonwood represent the combination of both on pectin and hemicelluloses. During cell wall biogenesis, the composition and architecture of the wall sequentially change. The matrix polysaccharide of primary cell wall pectin eventually is replaced by hemicelluloses in the secondary cell wall; meanwhile, the phenolic polymer lignin is deposited and integrated into the wall matrix (Carpita and McCann 2000). The developmentally changed acetylesterification of cell wall suggests that *O*-acetylation might be important for the macromolecular organization, metabolism, and function of the cell wall polysaccharides in vivo.

Compared to acetylester, the "wall-bound" phenolics and their putative dehydrodimers in poplar display more conspicuous tissue-specific accumulation and developmental changes. The accumulations of *p*-coumarate and ferulate are clearly distinguishable, and the patterns are diametrically opposite in the stems under normal growth condition (Figs. 4, 5). These results implicate their potentially different functions in the cell-wall biogenesis and structural construction. In the cell walls of grasses, the ferulate linked on non-cellulosic polysaccharides is thought to be mainly responsible for cross-linking polysaccharide–polysaccharide or polysaccharide–lignin through peroxidase-catalyzed dehydrodimerization (Ralph et al. 2004). The content of ferulate and its putative dimers in poplar's cell wall increased gradually from developing stems to more "woody" stems (Figs. 4c, d, 5), denoting that ferulate is involved in constructing the poplar secondary cell wall, as it is in the cell wall of grass. Previous studies demonstrated that the level of *p*-coumarate in the cell wall of grass is less than that of ferulate and it is incorporated into the wall mainly through modifying monolignols (Ralph et al. 2004). Unlike ferulate that serves as a cross-linker of polysaccharide, *p*-coumarate likely acts as an 'oxidation catalyst' mediating radical transfer to promote the dehydrodimerization of monolignol sinapyl alcohol during lignification of the cell wall of grasses (Ralph et al. 2004). Interestingly, in poplar, *p*-coumarate was a predominant acyl component in cell wall of juvenile leaf tissues and young stems (Fig. 4a, c) and its level fell along the development of stems (Fig. 5). Apparently, the cell walls of these young stem or leaf tissues were less lignified (Fig. 2c) and the cells in such tissues may contain principally primary cell wall. Together, these data may suggest that the function of the *p*-coumarate in cell wall of the dicot poplar might differ from its predicted role in lignifications of secondary cell wall in grass. *p*-Coumarate and ferulate may be both primarily involved in modifying cell wall non-cellulosic polysaccharides, but function distinctly in cell wall differentiation.

The accumulation of the "wall-bound" phenolics in the induced tension wood was decreased while acetate remains unchanged (Table 1). Tension wood is asymmetrically induced on the one side of the stem, in which it generally accumulates more highly crystalline cellulose microfibrils and a reduced amount of matrix carbohydrates and lignin (Timell 1969). During the formation of tension wood in poplar, hemicellulose and lignin biosyntheses decreased (Andersson-Gunneras et al. 2006). As two types of substituents to hemicellulose and lignin, the "wall-bound" phenolics might decrease directly in respect to the reduced deposition of those matrix biopolymers. Alternatively, the induction of tension wood by altering a series of biochemical processes may down-regulate the enzymatic esterification of phenolics to the cell wall matrix components. During the decline of the "wall-bound" phenolics, the level of the wall-associated acetate in tension wood remains generally constant. Considering the reduction of cell wall matrix biopolymers in the reactive tension wood tissues, maintaining the constant level of acetate implicates a potential induction of the acetylesterification to the hemicellulose and/or lignin by the bending treatment.

Finally, in current study we explored the application of FT-IR and synchrotron IR spectroscopic imaging techniques in detecting and anatomically localizing cell wall compositions, primarily the (acyl)ester compositions in poplar tissues. With the characteristic infrared absorptions of many functional groups of cell wall compositions (McCann et al. 2001; Mouille et al. 2003), synchrotron IR spectroscopic imaging might be a valuable tool in examining the spatial distribution of cell wall components. Those techniques could be further applied into the rapidly anatomically screening cell wall mutant plants or dissecting the altered cell wall compositions of transgenic plants in cellular/subcellular level.

Acknowledgments The authors would like to thank Dr. Gray Tuskan in Oak Ridge National Laboratory for providing additional *P. trichocarpa* plantlets. This work was supported by the DOE-USDA joint Plant Feedstock Genomics Program (Project No. Bo-135) and the Laboratory Directed Research and Development Program (LDRD-07-047) of Brookhaven National Laboratory under contract with Department of Energy to Chang-Jun Liu. Use of the National Synchrotron Light source was supported by the U.S. Department of Energy, Office of Science, Office of Basic Energy Sciences, under Contract No. DE-AC02-98CH10886.

References

Andersson-Gunneras S, Mellerowicz EJ, Love J, Segerman B, Ohmiya Y, Coutinho PM, Nilsson P, Henrissat B, Moritz T, Sundberg B (2006) Biosynthesis of cellulose-enriched tension wood in *Populus*: global analysis of transcripts and metabolites identifies biochemical and developmental regulators in secondary wall biosynthesis. Plant J 45:144–165

Aspeborg H, Schrader J, Coutinho PM, Stam M, Kallas A, Djerbi S, Nilsson P, Denman S, Amini B, Sterky F, Master E, Sandberg G, Mellerowicz E, Sundberg B, Henrissat B, Teeri TT (2005) Carbohydrate-active enzymes involved in the secondary cell wall biogenesis in hybrid aspen. Plant Physiol 137:983–997

Biely P, MacKenzie CR, Puls J, Schneider H (1986) Cooperativity of esterases and xylanases in the enzymatic degradation of acetyl xylan. Biotechnology 4:731–733

Bunzel M, Ralph J, Lu F, Hatfield RD, Steinhart H (2004) Lignins and ferulate-coniferyl alcohol cross-coupling products in cereal grains. J Agric Food Chem 52:6496–6502

Carpita NC, McCann MC (2000) The cell wall. In: Buchanan BB, Gruissem W, Jones RL (eds) Biochemistry and molecular biology of plants. American Society of Plant Physiologists, Rockville, pp 52–108

Croteau R, Kutchan TM, Lewis NG (2000) Natural products (secondary metabolites). In: Buchanan BB, Gruissem W, Jones RL (eds) Biochemistry and molecular biology of plants. American Society of Plant Physiologists, Rockville, pp 1250–1318

Franke R, Hemm MR, Denault JW, Ruegger MO, Humphreys JM, Chapple C (2002) Changes in secondary metabolism and deposition of an unusual lignin in the *ref8* mutant of *Arabidopsis*. Plant J 30:47–59

Fry SC (1986) Cross-linking of matrix polymers in the growing cell walls of angiosperms. Annu Rev Plant Physiol Plant Mol Biol 37:165–186

Fry SC, Miller JC (1989) Toward a working model of the growing plant cell wall. Phenolic cross-linking reactions in the primary cell walls of dicotyledons. In: Lewis NG, Paice MG (eds) Plant cell wall polymers, biogenesis and biodegradation, vol 399. American Chemical Society, Washington, DC, pp 33–46

Grabber JH, Ralph J, Lapierre C, Barrière Y (2004) Genetic and molecular basis of grass cell-wall degradability. I. Lignin–cell wall matrix interactions. C R Biol 327:455–465

Hatfield RD, Ralph J, Grabber JH (1999) Cell wall cross-linking by ferulates and diferulates in grasses. J Sci Food Agric 79:403–407

Iiyama K, Lam TB-T, Stone BA (1994) Covalent cross-links in the cell wall. Plant Physiol 104:315–320

Ishii T (1997a) Structure and functions of feruloylated polysaccharides. Plant Sci 127:111–127

Ishii T (1997b) O-acetylated oligosaccharides from pectins of potato tuber cell walls. Plant Physiol 113:1265–1272

Jacobs A, Lundqvist J, Stalbrand H, Tjerneld F, Dahlmana O (2002) Characterization of water-soluble hemicelluloses from spruce and aspen employing SEC/MALDI mass spectroscopy. Carbohydr Res 337:711–717

Kacuráková M, Wellner N, Ebringerová A, Hromádková Z, Wilson RH, Belton PS (1999) Characterization of xylan-type polysaccharides and associated cell wall components by FT-IR and FT-Raman spectroscopies. Food Hydrocoll 13:35–41

Kacuráková CP, Sasinková V, Wellner EA (2000) FT-IR study of plant cell wall model compounds: pectic polysaccharides and hemicelluloses. Carbohydr Polym 43:195–203

Kato Y, Nevins DJ (1984) Enzymic dissociation of zea shoot cell wall polysaccharides: IV. Dissociation of glucuronoarabinoxylan by purified endo-(1 → 4)-β-xylanase from *Bacillus subtilis*. Plant Physiol 75:759–765

Kauppinen S, Christgau S, Kofod LV, Halkier T, Dörreich K, Dalbøge H (1995) Molecular cloning and characterization of a rhamnogalacturonan acetylesterase from *Aspergillus aculeatus*. J Biol Chem 270:27172–27178

Lam TBT, Kadoya K, Iiyama K (2001) Bonding of hydroxycinnamic acids to lignin: ferulic and *p*-coumaric acids are predominantly linked at the benzyl position of lignin, not the β-position, in grass cell walls. Phytochemistry 57:987–992

Liners F, Gaspar T, Van Cutsem P (1994) Acetyl- and methyl-esterification of pectins of friable and compact sugar-beet calli: consequences for intercellular adhesion. Planta 192:545–556

Lu FC, Ralph J (1999) Detection and determination of *p*-coumaroylated units in lignins. J Agric Food Chem 47:1988–1992

Lu FC, Ralph J (2002) Preliminary evidence for sinapyl acetate as a lignin monomer in kenaf. Chem Commun (Camb), pp 90–91

Marchessault RH, Liang CY (1962) The infrared spectra of crystalline polysaccharides. VIII. Xylans. J Polym Sci 59:357–378

McCann MC, Bush M, Milioni D, Sado P, Stacey NJ, Catchpole G, Defernez M, Carpita NC, Hofte H, Ulvskov P, Wilson RH, Roberts K (2001) Approaches to understanding the functional architecture of the plant cell wall. Phytochemistry 57:811–821

Miller LM, Dumas P (2006) Chemical imaging of biological tissue with synchrotron infrared light. Biochim Biophys Acta 1758:846–857

Mouille G, Robin S, Lecomte M, Pagant S, Hofte H (2003) Classification and identification of *Arabidopsis* cell wall mutants using Fourier-transform infrared (FT-IR) microspectroscopy. Plant J 35:393–404

Pauly M, Anderson LN, Kauppinen S, Kofod LV, York WS, Albersheim P, Darvill AG (1999) A xyloglucan-specific endo-β-1,4-glucanase from *Aspergillus aculeatus*: expression cloning in yeast, purification and characterization of the recombinant enzyme. Glycobiology 9:93–100

Philippe S, Robert P, Barron C, Saulnier L, Guillon F (2006) Deposition of cell wall polysaccharides in wheat endosperm during grain development: Fourier transform-infrared microspectroscopy study. J Agric Food Chem 54:2303–2308

Piber M, Koehler P (2005) Identification of dehydro-ferulic acid-tyrosine in rye and wheat: evidence for a covalent cross-link between arabinoxylans and proteins. J Agric Food Chem 53:5276–5284

Pippen EL, McCready RM, Owens HS (1950) Gelation properties of partially acetylated pectins. J Am Chem Soc 72:813–816

Ralph J, Bunzel M, Marita JM, Hatfield RD, Lu F, Kim H, Schatz PF, Grabber JH, Steinhart H (2004) Peroxidase dependent cross-linking reactions of *p*-hydroxycinnamates in plant cell walls. Phytochem Rev 3:79–96

Renard CC, Jarvis MC (1999) Acetylation and methylation of homogalacturonans 1: optimisation of the reaction and characterization of the products. Carbohydr Polym 39:201–207

Robert P, Marquis ML, Barron C, Guillon F, Saulnier L (2005) FT-IR investigation of cell wall polysaccharides from cereal grains. Arabinoxylan infrared assignment. J Agric Food Chem 53:7014–7018

Rombouts FM, Thibault JF (1986) Enzymatic and chemical degradation and the fine structure of pectins from sugar-beet pulp. Carbohydr Res 154:189–203

Schols HA, Voragen AG (1994) Occurrence of pectic hairy regions in various plant cell wall materials and their degradability by rhamnogalacturonase. Carbohydr Res 256:83–95

Sederoff RR, MacKay JJ, Ralph J, Hatfield RD (1999) Unexpected variation in lignin. Curr Opin Plant Biol 2:145–152

Teleman A, Lundqvist J, Tjerneld F, Stålbrand H, Dahlman O (2000) Characterization of acetylated 4-*O*-methylglucuronoxylan isolated from aspen employing 1H and 13C NMR spectroscopy. Carbohydr Res 329:807–815

Teleman A, Nordström M, Tenkanen M, Jacobs A, Dahlman O (2003) Isolation and characterization of *O*-acetylated glucomannans from aspen and birch wood. Carbohydr Res 338:525–534

Tenkanen M (1998) Action of *Trichoderma reesei* and *Aspergillus oryzae* esterases in the deacetylation of hemicelluloses. Biotechnol Appl Biochem Pt 1:19–24

Timell TE (1964) Wood hemicelluloses. Adv Carbohydr Chem 19:247–302

Timell TE (1969) The chemical composition of tension wood. Sven Papperstidn 72:173–181

Tuskan GA et al (2006) The genome of black cottonwood, *Populus trichocarpa* (Torr. & Gray). Science 313:1596–1604

Voragen AGJ, Pilnik W, Thibault J-F, Axelos MAV, Renard MGC (1998) Pectins. In: Dekker M (ed) Food polysaccharides and their applications. Academic Press, New York, pp 287–339

Wende G, Fry SC (1997a) 2-*O*-*β*-D-Xylopyranosyl-(5-*O*-feruloyl)-L-arabinose, a widespread component of grass cell walls. Phytochemistry 44:1019–1030

Wende G, Fry FC (1997b) *O*-feruloylated, *O*-acetylated oligosaccharides as side-chains of grass xylans. Phytochemistry 44:1011–1018

Williamson G, Faulds CB, Matthew JA, Archer DB, Morris VJ, Brownsey GJ, Ridout MJ (1990) Gelation of sugarbeet and citrus pectins using enzymes extracted from orange peel. Carbohydr Polym 13:387–397